CSI RD&D4 Task 3 Final Report

Granular Operational Net Load Forecasting.

Submitted to:
California Public Utilities Commission
California Solar Initiative RD&D Program

April 2016

Submitted by:
Yinghao Chu, Carlos Coimbra, Hugo Pedro
Department of Mechanical and Aerospace Engineering
Jacobs School of Engineering
Center for Renewable Resource Integration and Center for Energy Research
University of California, San Diego
9500 Gilman Drive
La Jolla, CA 92093-0411

Table of Contents

Abstract 1

Introduction 2

Methodologies 2

Error Metrics 5

Short-term forecasts 5

Day-ahead forecasts 7

ABSTRACT

Net load forecasts for 68 substations were developed and validated for forecast horizons ranging from 10 min to 4 days. The methods implemented include Artificial Neural Networks (ANN), Support Vector Regression (SVR), sky-imaging techniques, and other time series methods. The forecasting models were trained and validated using measurements of the net load and assessed using common statistic metrics (MAE and rRMSE). The assessment results show that stochastic-learning models significantly outperform the reference persistence model. These models were assembled into forecasting packages that are operational with real-time telemetry data.

INTRODUCTION

Distributed solar generation is growing rapidly due to the net energy metering tariffs and other incentives [1]. The variable rooftop solar generation adds substantial uncertainties in power demand at the substation level [2] and changes the variability of net load time series. In general, for operating regions with higher solar penetration levels, the variability in solar power production propagates into the load profile and increases the relative error of net load forecasts during the daytime.

Uncertainties in electric loads need to be compensated for using operating reserves or ancillary generation, which increase the overall costs for utilities, customers, system operators, and other market participants [3]. Short-term load forecasts play a key role in mitigating the uncertainty of loads and are essential to decrease the costs of operation, control, management, balancing and scheduling of the electric grid. For instance, intra-hour load forecasts are needed for real-time control and load following [4]. Day-ahead load forecasts are required by Independent System Operators (ISOs), utilities, and electricity market participants for operation planning and unit commitment of generating plants.

To accurately forecast the net load with the influence of distributed solar production, this work describes a methodology to reduce the uncertainty for all forecast horizons using two popular stochastic learning models: Artificial Neural Network (ANN) and Support Vector Machine (SVM). The developed forecasts are operational providing that there is robust real-time telemetry data available.

This methodology was applied to data from 68 substations. The developed forecasts for 68 substations were prepared in operational packages. The forecast packages were validated in real-time scenario using measured net-load data and the forecast performance was quantified in terms of Mean Absolute Error (MAE) and relative Root Mean Square Error (rRMSE) and is shown for each substation in the Appendix. The forecast results for four representative feeders (denoted as Feeder A, B, C, and D) are analyzed and presented in detail to demonstrate the general performance of the forecast packages.

METHODOLOGIES

The developed models were prepared in forecasting packages for all 68 substations. Each package includes all necessary function files, processing algorithms, and trained models to forecast the net loads. These forecasting packages are ready to be applied in real time operations. The forecast can be represent as:

$$\hat{L} = f(T, I_1, \dots, I_N, t_1, \dots, t_N),$$

where T is the time when the forecasting package is called and executed, f represents the forecasting function, I represents both endogenous and exogenous inputs, t represent the timestamps associated with the inputs, and $\hat{L}$ represents the prediction value. For the intra-hour packages, $\hat{L}$ are predictions of 1-minute averaged net loads for 10-, 20-, and 30-minute horizons. For the day-ahead packages, $\hat{L}$ are predictions of 1-hour averaged net loads for 1-, 2-, 3-, and 4-day horizons. In this work, the forecasts are produced using Artificial Neural Networks (ANN) and Support Vector Regression (SVR).

ANN and SVR are popular stochastic-learning tools for pattern recognition, data classification and regression, and have proven to be useful for non-linear input/output mapping [2, 3]. Therefore, both ANN and SVR are employed to implement the net load forecasts. The weights and parameters of both ANN and SVR are estimated using the training dataset.

The employed ANN places the basic processing elements (named neurons) in layers and allows only forward connections of the neurons. The layers between the first input layer and the last output layer are hidden layers.

Neurons take in weighted sum of inputs Xj through various layers and produce an output using an activation function.

$$Y_i = f\left(\sum_{j=1}^{N} w_{ij} X_j\right),$$

where the Y_i is the output from the i-th neuron, and f is an activation function. For this study, the structure of the ANN follows the optimized scheme that was obtained in previous work using a Genetic Algorithm (GA).

The SVR modeling uses inputs that are known as support vectors and can be mathematically expressed as

$$f(X) = < w, X > + b,$$

where w represents the weights and b is a constant. The optimization problem is solved with the following objective and constraints,

$$\min_{w,b,\xi,\xi^*} \frac{1}{2} w'w + C \sum_{i=1}^{l} (\xi_i + \xi_i^*)$$

$$\text{subject to } X_i - (w'f(X) + b) \leq \epsilon + \xi_i,$$

$$(w'f(X) + b) - X_i \leq \epsilon + \xi_i^*,$$

$$\xi_i, \xi_i^* \geq 0, i = 1, \dots, l,$$

where ξ_i, ξ_i^* are the upper and lower training errors subject to an ϵ-insensitive tube and C is the cost of the error. Therefore, the parameters C, ϵ, and the mapping function f control the regression quality obtained using SVR. A radial basis function was used as a mapping function while cross-validation was used to compute the other parameters [3].

The net load data used as input to the models explained above is preprocessed before being assimilated. In the real-time scenario, the net load data are not evenly sampled resulting in variable sampling intervals (Fig. 1). Consequently, the number of available endogenous inputs varies adversely affecting the performance of the forecasts. To overcome this issue an interpolation algorithm was developed and employed in each of the forecasting packages. The interpolation algorithm analyzes the input time series and interpolates a constant number of inputs to the forecasting package. This procedure significantly improves the robustness of the net load forecasts.

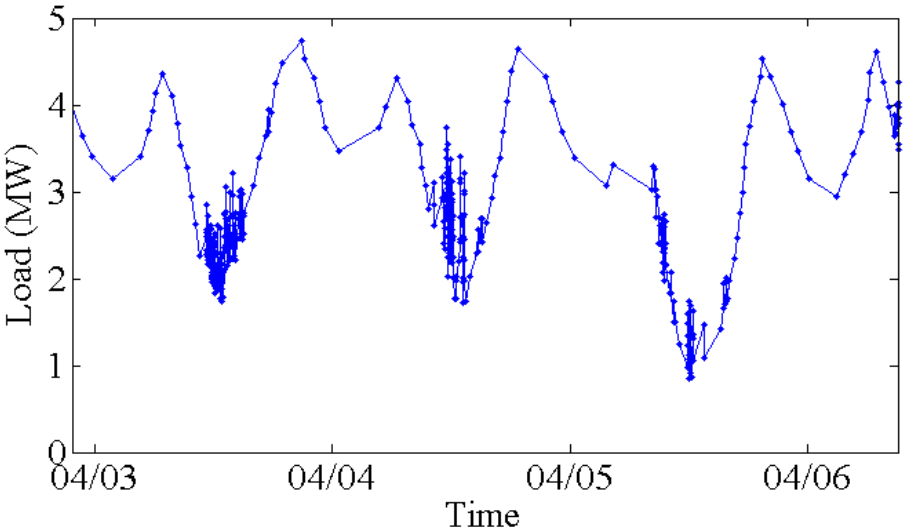

Figure 1: Sample time-series of net load recorded at the Feeder A illustrating a variable sampling rate.

The key inputs for intra-hour forecast consist of information retrieved from sky-images. The inputs are retrieved using an efficient image-processing algorithm [5]. This algorithm translates the sky images into numerical image features. These image features, which represent cloud cover information that are critical for determining short-term solar ramps, are used as inputs to the multi-layer stochastic learning forecast engine. The image-processing algorithm includes three major procedures: (1) image masks are manually annotated to exclude the ground obstacles (e.g. trees, buildings); (2) normalized red blue ratios (NRBRs) are calculated for each unmasked pixel; (3) image features (mean, std, entropy) for a sky image are statistically derived based on the NRBRs of all its unmasked pixels. Examples of the image processing are illustrated in Fig. 2. This algorithm is high-speed (less than 1 second for each sky image). With minimal adjustments it could be applied to images from different cameras e.g. as installed by the utility at substations.

The image-processing algorithm was applied to a UC San Diego Sky Imager (USI) located in Feeders A and B to create a database of sky image features. This database was created with images from October 2014 to May 2015. The database was used for both training and validation of the stochastic learning forecast engine. No sky imager data was used at the other 66 feeders. Also the sky imager was operated in 'resource assessment' mode, i.e., no solar forecast maps were generated from the images.

Treating weekdays and weekends separately did not result into improved forecasting performance. For this reason, the forecasting packages handle the input data always the same way regardless of the type of day the forecast is targeting.

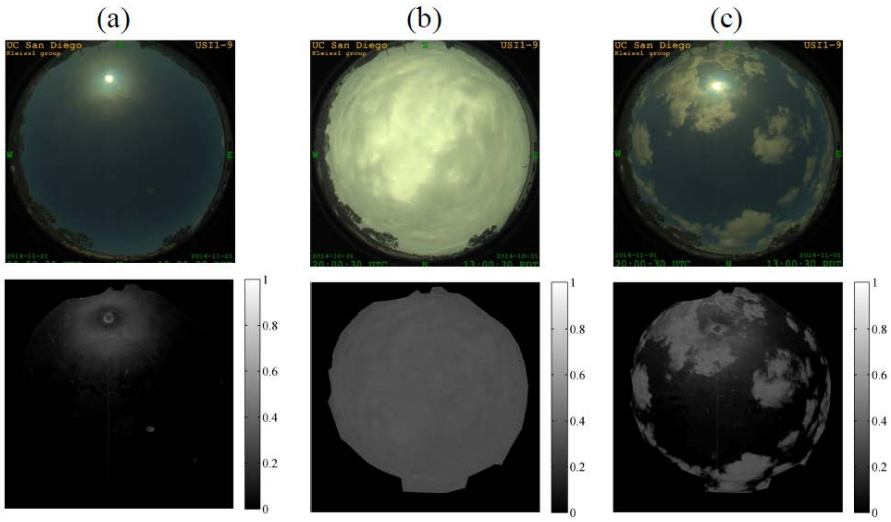

Figure 2: Examples of original images (top row) and normalized RBR (nRBR) images (bottom row) recorded at Feeder B, which are returned from the developed image-processing algorithm period. The gray scales indicate the nRBR magnitudes in each image.

ERROR METRICS

Two error metrics were used in this work to assess the forecast performance: Mean Absolute Error (MAE) and relative Root Mean Square Error (rRMSE). MAE is defined as:

$$\mathrm{MAE} = \frac{1}{n}\sum_{t=1}^{n}\left|\frac{\hat{L}_t - L_t}{L_t}\right|,$$

rRMSE gives the information about the spread i.e., standard deviation in the errors:

$$\mathrm{rRMSE} = \frac{\sqrt{\frac{1}{n}\sum_{t=1}^{n}\left(\hat{L}_t - L_t\right)^2}}{\frac{1}{n}\sum_{t=1}^{n}|L_t|},$$

where the denominator $\frac{1}{n}\sum_{t=1}^{n}|L_t|$ is the averaged value of net load.

Short-term forecasts

ANN and SVR short-term forecast packages were implemented for 10-, 20-, and 30-minute forecast horizons with 10-minute resolution. The forecast validation results for the 68 substations are presented in the Appendix in terms of MAE and rRMSE. The forecasts for four representative feeders are presented in this section in more detail to demonstrate the general performance of the forecast packages. The data used for intra-hour forecasts were collected between Oct. 2014 and Mar. 2015 and divided into two disjointed datasets: the training dataset (the first three weeks of each month) for model training/optimization and the validation dataset (the last week of each month) for model validation. Sky images are only available for two of the representative feeders; Feeders A and B and exogenous forecasts can only be applied there. For all other substations, we applied endogenous forecasts which consider only the substation power output time series. Baseline forecasts were developed using endogenous inputs only without employing sky-image inputs. The endogenous inputs are the lagged values of net load ranging from zero to one hour in steps of 10 minutes.

Sky images are only available during day time. Therefore, the comparisons of error metrics are limited to forecasts during day time. The comparison between sky-image enhanced forecasts and baseline forecasts in

terms of MAE and rRMSE is illustrated in Table 1. For Feeder A, the rRMSEs of forecasts with sky imagers (Im-ex) are averagely 4% lower than that of baseline forecasts. For Feeder B, the rRMSEs of Im-ex forecasts are averagely 5% lower than that of baseline forecasts. When Im-ex inputs are used, improvements in term of rRMSE for Feeder B are higher than that for Feeder C. This is expected because that the solar penetration level, which is defined as the annual solar energy produced divided by the annual total load on the feeder, of Feeder B is significantly higher than that of Feeder A. The overall solar penetration levels at both feeders are still very low (2.4% for Feeder C, and 5.8% for Feeder B). Therefore, Im-ex forecasts only achieve marginal improvements in term of rRMSE for these two feeders. The benefits of Im-ex inputs are expected to increase for feeders with higher level of solar penetration.

Table 1: MAE and rRMSE (daytime only) for reference persistence forecasts, baseline endogenous forecasts, and forecasts with image features as exogenous inputs for 10-, 20-, and 30- minute horizons. The investigated models are the ANN and SVR models. Note that only the two feeders with available sky imager data are included in this Table.

		Feeder A			**Feeder B**		
Forecast Horizon	[min.]	10	20	30	10	20	30
Per	MAE	0.020	0.037	0.052	0.020	0.035	0.049
	rRMSE	0.043	0.066	0.084	0.056	0.092	0.127
ANN	MAE	0.024	0.039	0.050	0.018	0.026	0.033
	rRMSE	0.040	0.059	0.071	0.044	0.063	0.080
ANN with Im-ex	MAE	0.025	0.037	0.042	0.018	0.024	0.028
	rRMSE	0.040	0.056	0.064	0.044	0.059	0.073
SVR	MAE	0.032	0.044	0.053	0.019	0.026	0.032
	rRMSE	0.044	0.060	0.072	0.045	0.063	0.079
SVR with Im-ex	MAE	0.027	0.038	0.043	0.020	0.026	0.029
	rRMSE	0.046	0.061	0.068	0.048	0.065	0.074

Example time-series of enhanced forecasts and corresponding absolute errors are shown in Fig. 3 for Feeder B for a period of 48 hours. The daytime forecasts consider image features as exogenous inputs while the nighttime forecasts uses only endogenous inputs. Feeder B has a solar penetration level of 5.79%, and the impact of solar variability on the net load time series can be seen in Fig. 3, particularly around noon when the solar power reaches its daily maximum. The improvement achieved using stochastic models with enhancement methods over the reference persistence model is noticeable and is clearly presented in the time series of forecast errors. The highest improvements are observed during midnight and early morning when the net load time series has a monotonous and smooth trend. During the middle of the days when exogenous inputs are available, both ANN and SVR forecasts achieve significantly lower error than the net load persistence forecasts.

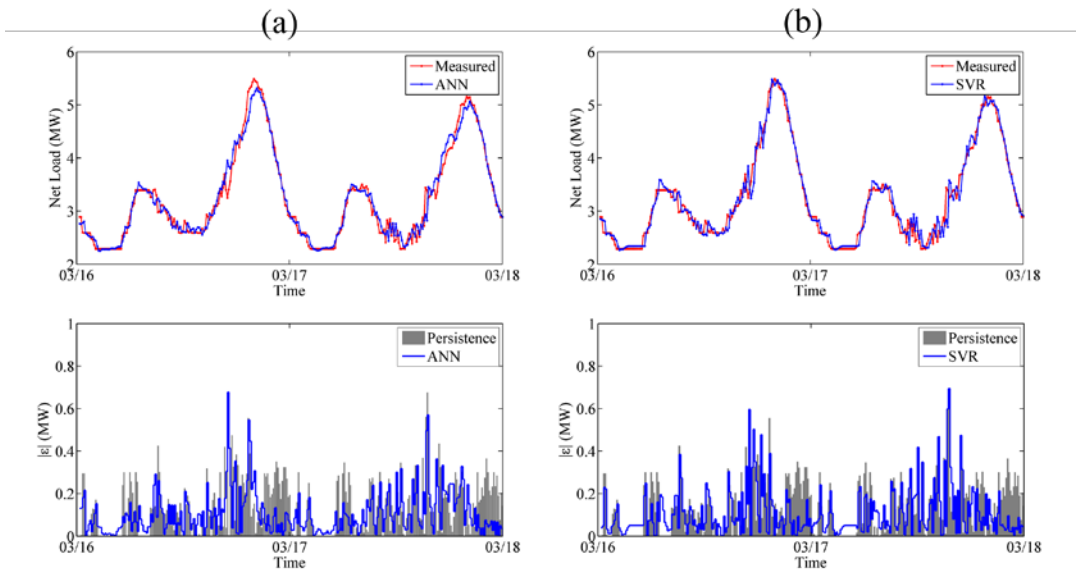

Figure 3: Sample time series of net load forecasts and absolute forecast errors (ε) for the Feeder B for a period of 48h using (a) ANN and (b) SVR. The timestamps indicate midnight (00:00) PDT.

Day-ahead forecasts

Day-ahead forecasts use different exogenous data than short-term forecasts. For long forecast horizons, sky images are not useful because cloud cover information derived from them is too short-lived. Instead, for day-ahead forecasts, the models use data from numerical weather prediction models. In this work, we use the solar irradiance and cloud cover forecasted by the North America Mesoscale Model (NAM). This model provides data on a 12 km x 12 km spatial grid that covers the continental United States. Forecasts are generated four times daily at 00Z, 06Z, 12Z and 18Z, with hourly temporal resolution for 1-36 h horizons and 3 h resolution for 39-84 h horizons. After downloading the data, we identify the NAM grid node closest to the feeders, extract the relevant variables and interpolate them to hourly time intervals coincident with the net load data. Using measured and NAM data the day-ahead ANN and SVR forecast models were developed and validated for the 68 substations for 1-, 2-, 3-, and 4-day forecast horizons with 1-hour resolution. All the day-ahead forecasting packages were validated using 1-year testing data and their forecast performance is presented in the Appendix.

The forecast performance in terms of MAE and RMSE are presented in Tables 2-5 for the four representative feeders. The persistence model is used as a baseline model to benchmark the implemented net load forecasting models. For all models, both the MAE and RMSE increase with the forecast horizon, regardless of the locations. For example, the persistence RMSE at the Feeder D increases from 0.178 to 0.235 (18% to 24%) when the forecast horizon increases from 1-day to 4-day. For all feeders, the stochastic learning models achieve error metrics that are significantly lower than the reference persistence model, particularly for longer horizon forecasts. For example at the Feeder A, the RMSE of 2-day ahead SVR forecasts is 0.428 and the RMSE for the persistence model is 0.522, an improvement of 18%. The sample time series of forecasts and corresponding errors for 2-day forecasts are presented in Fig 4. These figures clearly show the improvements of the stochastic learning models over the reference persistence models, particularly during periods of large ramps when persistence model has large errors.

Table 2: Net load forecasting results for 1 day forecast horizon for the four feeders.

		Persistence	ANN	SVR
MAE [-]	Feeder A	0.103	0.1	0.095
	Feeder B	0.054	0.053	0.052
	Feeder C	0.079	0.087	0.08
	Feeder D	0.094	0.086	0.087
rRMSE [-]	Feeder A	0.473	0.442	0.421
	Feeder B	0.267	0.253	0.249
	Feeder C	0.156	0.165	0.158
	Feeder D	0.178	0.16	0.166

Table 3: Net load forecasting results for 2 day forecast horizon for the four feeders.

		Persistence	ANN	SVR
MAE [-]	Feeder A	0.119	0.110	0.098
	Feeder B	0.066	0.062	0.060
	Feeder C	0.104	0.103	0.101
	Feeder D	0.118	0.102	0.106
rRMSE [-]	Feeder A	0.522	0.505	0.428
	Feeder B	0.330	0.308	0.293
	Feeder C	0.207	0.197	0.202
	Feeder D	0.225	0.196	0.204

Table 4: Net load forecasting results for 3 day forecast horizon for the four feeders.

		Persistence	ANN	SVR
MAE [-]	Feeder A	0.121	0.113	0.105
	Feeder B	0.070	0.067	0.064
	Feeder C	0.110	0.110	0.107
	Feeder D	0.122	0.109	0.110
rRMSE [-]	Feeder A	0.516	0.502	0.444
	Feeder B	0.352	0.343	0.311
	Feeder C	0.217	0.215	0.215
	Feeder D	0.240	0.214	0.217

Table 5: Net load forecasting results for 4 day forecast horizon for the four feeders.

		Persistence	ANN	SVR
MAE [-]	Feeder A	0.141	0.124	0.116
	Feeder B	0.073	0.066	0.064
	Feeder C	0.112	0.115	0.110
	Feeder D	0.117	0.114	0.110
rRMSE [-]	Feeder A	0.609	0.540	0.490
	Feeder B	0.369	0.339	0.315
	Feeder C	0.225	0.234	0.229
	Feeder D	0.235	0.228	0.221

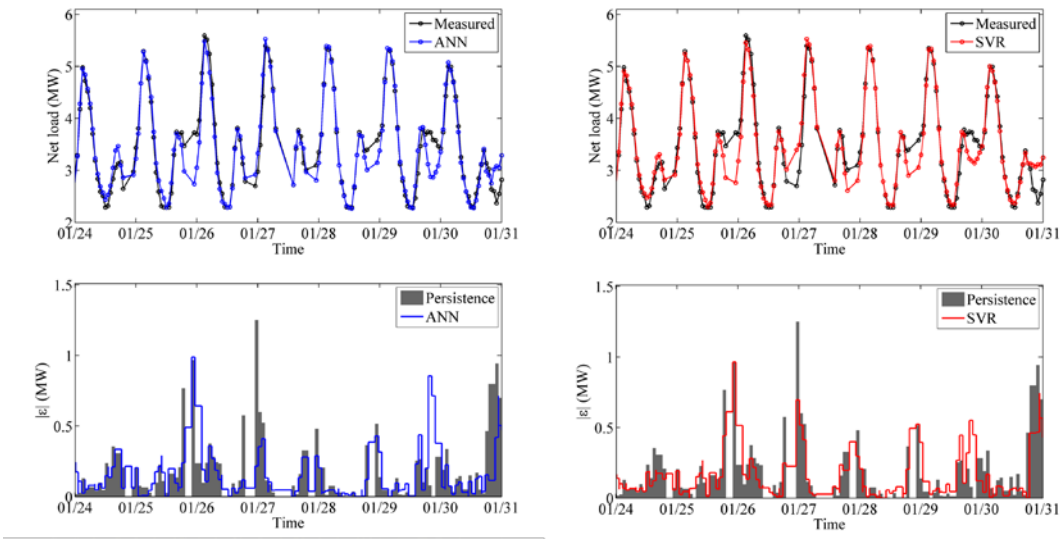

Figure 4: Sample time series of 2-day ahead net load forecasts (top row) and absolute forecast errors (bottom row) for the Feeder B for a period of 1-week using ANN (left column) and SVR (right column). Persistence forecast errors are shown for reference in grey. The timestamps are in UTC.

The forecast packages are implemented in real-time for four representative SDG&E feeders (A, B, C, and D). The online-demonstration of the forecasts is available at:

http://132.239.222.136/CSI4/DayAhead_Forecasts.html (real-time update of these forecasts depends on the availability of real-time data). Operational forecasting was live for about 2 months and frequent issues with the PI server administration prevented longer operational testing.

Conclusions

Net-load forecast for intra-hour and multiple day-ahead forecasts were successfully developed for the 68 substations in the SDG&E operating region. The models were assembled into forecasting packages that are operational. The very small latency times allows for producing operational forecasts given that robust real-time telemetry data is available from each substation. Advanced enhancement methods such as interpolation and image-processing algorithms were implemented to enhance the performance of forecasts. The models were validated using measured net load data showing that they outperform the baseline models in terms of MAE and rRMSE.

References

[1] A. Kaur, H. T. C. Pedro, C. F. M. Coimbra, Impact of onsite solar generation on system load demand forecast, Energy Conversion and Management 75 (2013) 701–709.

[2] P. Denholm, R. M. Margolis, Evaluating the limits of solar photovoltaics (PV) in electric power systems utilizing energy storage and other enabling technologies, Energy Policy 35 (9) (2007) 4424–4433.

[3] M. A. Ortega-Vazquez, D. S. Kirschen, Economic impact assessment of load forecast errors considering the cost of interruptions, in: Power Engineering Society General Meeting, 2006. IEEE, IEEE, 8–pp, 2006.

[4] A. Kaur, H. T. C. Pedro, C. F.M. Coimbra, Ensemble re-forecasting methods for enhanced power load prediction, Energy Conversion and Management 80 (2014) 582–590.

[5] H.T.C. Pedro and C.F.M. Coimbra, Nearest-Neighbor Methodology for Prediction of Intra-Hour Global Horizontal and Direct Normal Irradiances, Renewable Energy 80 (2015) 770-782.

Appendix

Table A-1: Intra-hour net load forecasting results for all 68 feeders, net load data is not available for location 17, 45, and 55.

	MAE [-]			rRMSE [-]		
Locations	10-min	20-min	30-min	10 min	20 min	30 min
1	0.02	0.04	0.05	0.04	0.06	0.07
2	0.06	0.14	0.15	0.06	0.09	0.11
3	0.01	0.02	0.03	0.04	0.07	0.09
4	0.01	0.02	0.03	0.04	0.08	0.10
5	0.03	0.04	0.05	0.07	0.10	0.13
6	0.02	0.02	0.03	0.05	0.07	0.09
7	0.01	0.02	0.02	0.05	0.09	0.12
8	0.07	0.11	0.12	0.11	0.15	0.18
9	0.01	0.02	0.03	0.04	0.07	0.09
10	0.03	0.04	0.05	0.11	0.15	0.19
11	0.01	0.02	0.02	0.07	0.10	0.12
12	0.01	0.01	0.02	0.04	0.07	0.10
13	0.02	0.03	0.04	0.05	0.08	0.10
14	0.01	0.02	0.02	0.03	0.04	0.05
15	0.01	0.01	0.01	0.03	0.05	0.07
16	0.01	0.01	0.02	0.04	0.06	0.07
17	NaN	NaN	NaN	NaN	NaN	NaN
18	0.01	0.02	0.02	0.06	0.09	0.11
19	0.01	0.02	0.02	0.07	0.09	0.12
20	0.05	0.12	0.15	0.08	0.10	0.11
21	0.03	0.05	0.06	0.06	0.10	0.12
22	0.03	0.05	0.06	0.07	0.10	0.13
23	0.01	0.01	0.02	0.04	0.05	0.06
24	0.01	0.01	0.02	0.04	0.07	0.10
25	0.01	0.01	0.03	0.04	0.08	0.14
26	0.01	0.02	0.02	0.06	0.15	0.17
27	0.01	0.02	0.05	0.05	0.09	0.14
28	0.01	0.01	0.02	0.04	0.07	0.09
29	0.01	0.01	0.02	0.04	0.06	0.08
30	0.01	0.01	0.02	0.03	0.05	0.06
31	0.01	0.01	0.02	0.03	0.05	0.06
32	0.01	0.02	0.02	0.05	0.08	0.11
33	0.07	0.11	0.12	0.04	0.08	0.10
34	0.07	0.07	0.06	0.04	0.07	0.09
35	0.01	0.02	0.02	0.04	0.07	0.09
36	0.01	0.01	0.01	0.07	0.09	0.13
37	0.01	0.01	0.01	0.04	0.06	0.09
38	0.01	0.01	0.01	0.03	0.05	0.07

	MAE [-]			rRMSE [-]		
Locations	10-min	20-min	30-min	10 min	20 min	30 min
39	0.01	0.01	0.01	0.04	0.06	0.07
40	0.01	0.02	0.02	0.09	0.10	0.12
41	0.01	0.02	0.02	0.06	0.13	0.15
42	0.01	0.02	0.02	0.07	0.11	0.13
43	0.03	0.04	0.05	0.05	0.06	0.08
44	0.01	0.02	0.02	0.07	0.11	0.12
45	NaN	NaN	NaN	NaN	NaN	NaN
46	0.01	0.02	0.02	0.07	0.13	0.16
47	0.02	0.03	0.03	0.05	0.07	0.08
48	0.01	0.01	0.02	0.03	0.04	0.06
49	0.01	0.02	0.02	0.03	0.05	0.06
50	0.02	0.03	0.03	0.05	0.08	0.10
51	0.01	0.01	0.02	0.05	0.07	0.09
52	0.01	0.01	0.02	0.04	0.07	0.10
53	0.01	0.02	0.02	0.08	0.08	0.09
54	0.01	0.02	0.02	0.04	0.06	0.08
55	NaN	NaN	NaN	NaN	NaN	NaN
56	0.01	0.02	0.02	0.06	0.08	0.10
57	0.01	0.02	0.02	0.05	0.08	0.11
58	0.01	0.02	0.03	0.06	0.09	0.11
59	0.01	0.02	0.02	0.05	0.08	0.11
60	0.01	0.02	0.02	0.12	0.13	0.11
61	0.01	0.02	0.02	0.03	0.05	0.07
62	0.04	0.05	0.06	0.16	0.24	0.19
63	0.01	0.02	0.02	0.05	0.12	0.16
64	0.00	0.01	0.01	0.03	0.04	0.06
65	0.01	0.02	0.02	0.06	0.10	0.12
66	0.05	0.12	0.15	0.09	0.14	0.16
67	0.04	0.05	0.06	0.07	0.14	0.15
68	0.04	0.06	0.07	0.07	0.10	0.12

Table A-2: Day-ahead net load forecasting results for all 68 feeders, net load data is not available for location 17, 45, and 55.

	MAE [-]				rRMSE [-]			
Location	1 day	2 day	3 day	4 day	1 day	2 day	3 day	4 day
1	0.11	0.15	0.16	0.17	0.18	0.24	0.27	0.27
2	0.12	0.14	0.15	0.15	0.24	0.32	0.35	0.39
3	0.08	0.11	0.13	0.13	0.28	0.40	0.47	0.49
4	0.08	0.11	0.12	0.13	0.28	0.40	0.46	0.49
5	0.17	0.21	0.23	0.22	0.34	0.43	0.46	0.46
6	0.09	0.11	0.13	0.14	0.37	0.41	0.43	0.47
7	0.09	0.10	0.10	0.11	0.38	0.40	0.43	0.47
8	0.09	0.11	0.13	0.14	0.44	0.56	0.61	0.63
9	0.07	0.09	0.10	0.10	0.25	0.31	0.33	0.34
10	0.08	0.12	0.13	0.14	0.40	0.53	0.60	0.63
11	0.06	0.08	0.09	0.09	0.31	0.42	0.46	0.47
12	0.05	0.07	0.08	0.08	0.29	0.40	0.44	0.45
13	0.06	0.08	0.09	0.09	0.16	0.19	0.21	0.22
14	0.04	0.05	0.06	0.06	0.12	0.15	0.17	0.17
15	0.04	0.06	0.07	0.07	0.20	0.28	0.32	0.33
16	0.04	0.06	0.07	0.07	0.21	0.29	0.33	0.34
17	NaN	NaN	NaN	NaN	NaN	NaN	NaN	NaN
18	0.08	0.10	0.11	0.11	0.38	0.45	0.50	0.51
19	0.08	0.10	0.11	0.11	0.38	0.45	0.50	0.52
20	0.12	0.14	0.15	0.15	0.36	0.44	0.46	0.46
21	0.20	0.23	0.26	0.27	0.37	0.41	0.47	0.47
22	0.21	0.25	0.27	0.28	0.38	0.43	0.47	0.48
23	0.04	0.05	0.06	0.06	0.14	0.19	0.21	0.21
24	0.06	0.08	0.08	0.08	0.31	0.37	0.39	0.41
25	0.09	0.11	0.13	0.14	0.36	0.42	0.44	0.43
26	0.07	0.09	0.09	0.09	0.38	0.45	0.48	0.51
27	0.07	0.09	0.10	0.10	0.25	0.31	0.33	0.34
28	0.07	0.09	0.09	0.09	0.35	0.41	0.44	0.45
29	0.07	0.08	0.09	0.10	0.37	0.42	0.47	0.49
30	0.04	0.06	0.06	0.06	0.18	0.24	0.27	0.27
31	0.04	0.06	0.06	0.07	0.18	0.24	0.27	0.28
32	0.09	0.12	0.13	0.13	0.42	0.51	0.57	0.61
33	0.09	0.11	0.13	0.14	0.42	0.50	0.57	0.60
34	0.11	0.12	0.13	0.14	0.25	0.31	0.33	0.34
35	0.09	0.11	0.13	0.14	0.45	0.54	0.62	0.67
36	0.06	0.07	0.08	0.08	0.32	0.39	0.42	0.43
37	0.06	0.07	0.08	0.08	0.30	0.37	0.40	0.41
38	0.06	0.07	0.08	0.08	0.30	0.37	0.41	0.41
39	0.06	0.07	0.08	0.08	0.30	0.36	0.40	0.41

	MAE [-]				rRMSE [-]			
Location	1 day	2 day	3 day	4 day	1 day	2 day	3 day	4 day
40	0.04	0.06	0.07	0.07	0.25	0.33	0.36	0.35
41	0.05	0.07	0.07	0.07	0.29	0.37	0.41	0.40
42	0.06	0.07	0.08	0.07	0.33	0.40	0.43	0.41
43	0.09	0.13	0.14	0.15	0.15	0.21	0.24	0.25
44	0.12	0.14	0.15	0.15	0.24	0.27	0.28	0.28
45	NaN	NaN	NaN	NaN	NaN	NaN	NaN	NaN
46	0.07	0.09	0.11	0.12	0.34	0.46	0.51	0.51
47	0.05	0.07	0.07	0.08	0.13	0.17	0.19	0.20
48	0.05	0.07	0.07	0.08	0.15	0.21	0.24	0.25
49	0.06	0.09	0.09	0.09	0.18	0.25	0.27	0.27
50	0.10	0.13	0.14	0.14	0.29	0.36	0.39	0.40
51	0.07	0.09	0.10	0.10	0.32	0.44	0.48	0.49
52	0.07	0.10	0.11	0.11	0.34	0.46	0.51	0.51
53	0.09	0.12	0.12	0.12	0.38	0.47	0.50	0.51
54	0.09	0.12	0.12	0.12	0.36	0.47	0.50	0.51
55	NaN	NaN	NaN	NaN	NaN	NaN	NaN	NaN
56	0.07	0.10	0.11	0.11	0.36	0.49	0.56	0.59
57	0.07	0.09	0.10	0.10	0.37	0.49	0.56	0.59
58	0.08	0.10	0.11	0.12	0.35	0.46	0.54	0.57
59	0.08	0.10	0.12	0.12	0.36	0.47	0.54	0.57
60	0.07	0.09	0.11	0.11	0.30	0.41	0.46	0.48
61	0.06	0.09	0.10	0.11	0.28	0.40	0.46	0.48
62	0.05	0.07	0.08	0.08	0.30	0.36	0.40	0.39
63	0.07	0.10	0.11	0.11	0.35	0.43	0.48	0.47
64	0.05	0.06	0.07	0.07	0.26	0.33	0.36	0.36
65	0.06	0.07	0.08	0.08	0.31	0.36	0.39	0.40
66	0.10	0.13	0.14	0.14	0.37	0.46	0.50	0.50
67	0.12	0.14	0.15	0.15	0.36	0.45	0.50	0.50
68	0.11	0.14	0.16	0.17	0.17	0.22	0.25	0.26